Structural Integrity Assessment Using In-Situ Acoustic Emission Monitoring

Masoud Rabiei[1], Mohammad Modarres[2], and Paul Hoffman[3]

[1]*Impact Technologies, Rochester, NY, 14623, USA*
masoud.rabiei@impact-tek.com

[2]*University of Maryland, College Park, MD, 20742, USA*
modarres@umd.edu

[3]*NAVAIR 4.3.3 Structures Division, Patuxent River, MD 20670, USA*
paul.hoffman@navy.mil

ABSTRACT

The work presented in this paper is focused on monitoring fatigue crack growth in metallic structures using acoustic emission (AE) technology. Three different methods are proposed to utilize the information obtained from in-situ monitoring for structural health management.

Fatigue crack growth tests with real-time acoustic emissions monitoring are conducted on CT specimens made of 7075 aluminum. Proper filtration of the resulting AE signals reveals a log-linear relationship between fracture parameters (da/dN and ΔK) and select AE features; a flexible statistical model is developed to describe the relationship between these parameters.

Bayesian inference is used to estimate the model parameters from experimental data. The model is then used to calculate two important quantities that can be used for structural health management: (a) an AE-based instantaneous damage severity index, and (b) an AE-based estimate of the crack size distribution at a given point in time, assuming a known initial crack size distribution.

Finally, recursive Bayesian estimation is used for online integration of the structural health assessment information obtained from AE monitoring with crack size estimates obtained from empirical crack growth model. The evidence used in Bayesian updating includes observed crack sizes and/or crack growth rate observations.

---

1. INTRODUCTION

Acoustic emissions are elastic stress waves generated by a rapid release of energy from localized sources within a material under stress (Mix 2005). Acoustic emissions often originate from defect-related sources such as permanent microscopic deformation within the material and fatigue crack extension.

Despite significant improvements in AE technology in recent years, quantitative interpretation of the AE signals and establishing a correlation between them and the source events remains a challenge and a topic for active research. In recent years, AE research has focused on two main areas; the first area has to do with characterizing the wave propagation through complex geometries which has proved to be an extremely difficult problem. The second area of research is concerned with processing the AE waveforms in an intelligent way (depending on the application) in order to extract useful information that can be traced back to the source event (Holford et al. 2009). The approach presented in this paper is in line with the second area.

In the first part of this paper, the problem of monitoring fatigue crack growth using AE technique is investigated. A statistical model is developed that correlates important crack growth parameters, i.e., crack growth rate, da/dN, and stress intensity factor range, ΔK, with select AE features. Next, this model will be used to calculate two important quantities that can be used for structural health management: (a) an AE-based instantaneous damage severity index, and (b) an AE-based estimate of the crack size distribution at a given point in time, assuming a known initial crack size distribution. Finally, the outcome of the statistical model described above will be used as direct "evidence" in a recursive Bayesian estimation framework to

update the model parameters as well as the estimated crack size distribution.

2. CRACK GROWTH MONITORING USING ACOUSTIC EMISSION

Fatigue crack growth is a well-known source of acoustic emission inside materials. Several researchers have studied the connection between fatigue crack growth behavior and the resulting acoustic emissions (Hamel et al. 1981; Bassim et al. 1994). Certain features of acoustic emission signals are found to be stochastically correlated with key fatigue parameters, such as stress intensity factor range, ΔK, and crack growth rate, da/dN. Two of the most commonly used AE parameters in fatigue are the AE count c and its derivative, count rate dc/dN. For a given AE signal, c is defined as the number of times that the signal amplitude exceeds a predefined threshold value. Accordingly, dc/dN is defined as the derivative of c with respect to time (measured as elapsed fatigue cycles).

The following form has been proposed by (Bassim et al. 1994) for the relationship between dc/dN and ΔK:

$$\frac{dc}{dN} = A_1 (\Delta K)^{A_2} \tag{1}$$

where A_1 and A_2 are the model parameters. Our goal is to use the AE parameter as the predictor to estimate the fatigue parameter; therefore, Eq. (1) is solved for ΔK and linearized as follows (Rabiei et al. 2009):

$$\log \Delta K = \alpha_1 \log \left(\frac{dc}{dN} \right) + \alpha_2 \tag{2}$$

where $\alpha_1 = A_1^{-1/A_2}$ and $\alpha_2 = 1/A_2$ are the new model constants to be estimated from data.

The significance of Eq. (2) is that once the model parameters are determined experimentally, this equation can be used to estimate ΔK by monitoring the acoustic emissions and extracting the dc/dN parameter from the observed signals—thus obviating the need for complex modeling and calculations used in fracture mechanics to calculate ΔK.

The second parameter that will be estimated via AE monitoring is the crack growth rate, da/dN. Based on the Paris equation (Paris & Erdogan 1963), da/dN is expected to have a log-linear relationship with ΔK while the crack growth is in the stable region. According to Eq. (2), ΔK itself has a log-linear relationship with dc/dN, which results in the following equation:

$$\log \left(\frac{da}{dN} \right) = \beta_1 \log \left(\frac{dc}{dN} \right) + \beta_2 \tag{3}$$

where β_1 and β_2 are the model parameters that describe the log-linear relationship between da/dN and dc/dN. From a structural monitoring perspective, this relationship means that on average, the rate of crack growth can be estimated solely based on features extracted from AE signals. This is a significant outcome because by knowing the rate of the crack growth and the initial crack size, the size of the crack can be estimated at any given time without knowing the specific load history or complex ΔK calculations. This fact will be used to develop an AE-based crack growth model that can predict the crack size as a function of observed AE signals.

2.1. Experimental test setup and procedure

A series of experiments were designed to validate the proposed relationship in Eqs. (2) and (3) and to generate the experimental data required for fitting the statistical model that will be introduced in the next section.

The experiments consisted of two separate parts that ran in parallel: the first part is a standard fatigue crack growth test in which a notched aluminum specimen undergoes cyclic loading, which causes a crack to initiate from the notch and grow until fracture; the second part is real-time AE monitoring—on the same specimen and while the crack is growing—to capture the AE signals resulting from the propagation of the crack inside the material.

Fatigue tests were carried out on standard compact tension (CT) specimens (ASTM E647-08 2008) made of 7075 aluminum alloy. The test setup is shown in Figure 1. The goal of the experiment was to record the AE signals generated by fatigue crack growth. To do so, we used a PCI-2 AE monitoring system supplied by Physical Acoustic Corporations[1] to monitor the CT specimen during the crack growth test. The most crucial step in AE monitoring is to distinguish the AE signals originating from the source event of interest (e.g. crack tip) from extraneous noises.
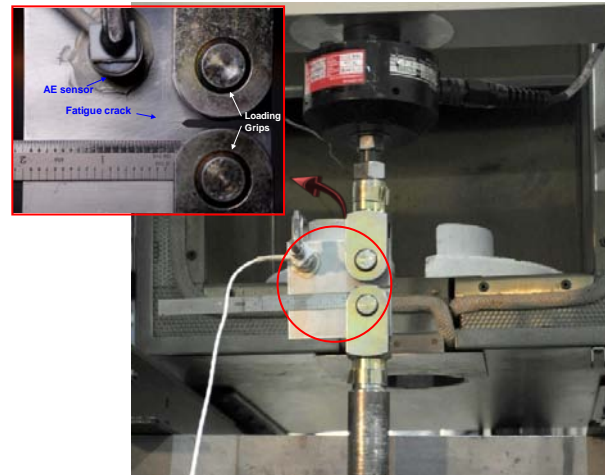

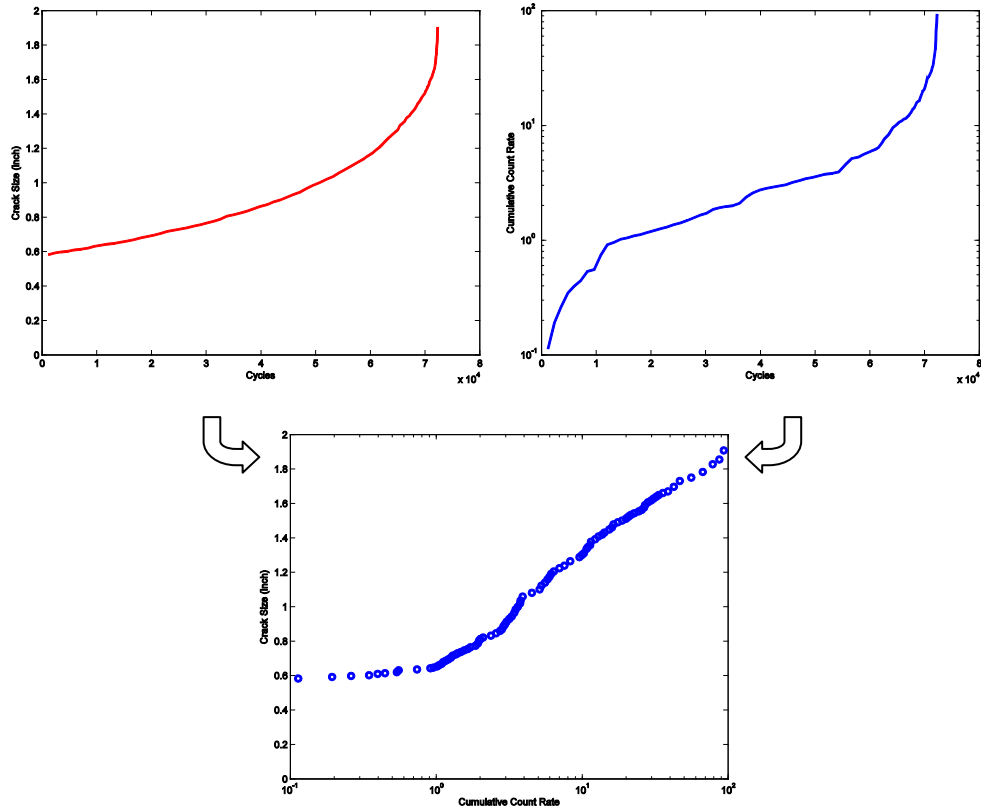Figure 1: CT specimen instrumented with AE sensor and mounted on MTS machine

---

[1] http://www.pacndt.com

Figure 2: Cumulative AE count rate versus crack size
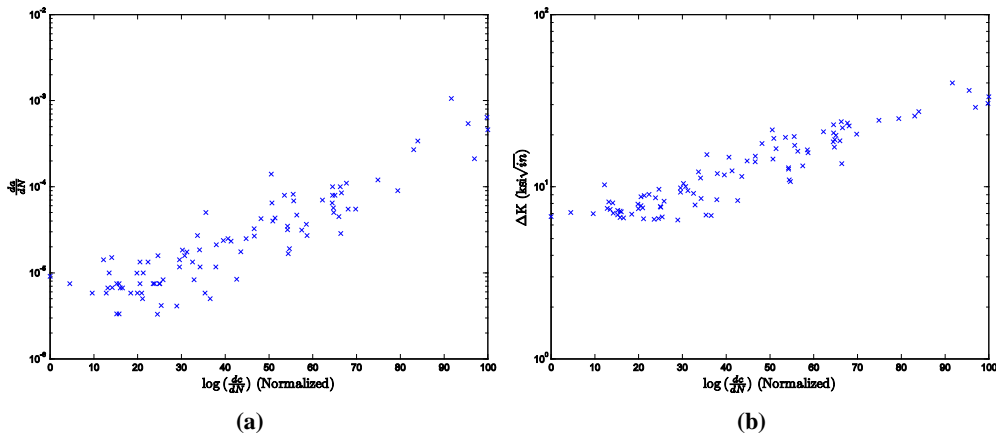

(a)

(b)

Figure 3: The linear correlation observed between dc/dN and da/dN (a) and ΔK (b) in a crack growth test

The source of the noise can be both internal (e.g., surface rubbing at loading pins, internal rubbing of crack surfaces) and external (e.g., noise from the hydraulic loading actuators). Various de-noising techniques were used to distinguish AE signals from the background noise. See (Rabiei 2011) for detailed information about the fatigue test setup, crack measurement technique and proper AE filtrations in crack growth monitoring.

Once proper filtration has been applied to the signals, the correlation between AE and crack growth parameters can be seen. Figure 2 shows that the increasing trend in crack size has a linear relationship with the cumulative AE count rate (on a log scale) for cracks larger than 0.6 inches. This suggests that in theory, the crack size can be measured by monitoring the cumulative AE count rate, if the relationship between the two is fully characterized and modeled.

Figure 3 shows the correlation between the AE parameter, dc/dN, and the fatigue parameters da/dN (a) and ΔK (b) on a log-log scale. These are the same data shown in Figure 2 but presented here in terms of derivatives. The linear correlation between fatigue and AE parameters is evident in this figure.

The dataset collected using the experimental procedure described here will be used to build a statistical model that can be used for AE-based structural health management.

2.2. Statistical model development

It was shown that on average, a log-linear relationship can be assumed between fracture parameters (da/dN or ΔK) and AE parameter (dc/dN). A statistical model is developed to describe the relationship between these parameters.

Let X denote dc/dN as the independent variable in the regression analysis, and Y denote either da/dN or ΔK as the dependent variable that we are interested in estimating. Regression analysis estimates the conditional expectation of the dependent variable given the independent variable — that is, the average value of the dependent variable when the independent variable is fixed. Another way of looking at this problem is to partition the dependent variable Y into a deterministic component given by function $\phi(\cdot)$ of the independent variable X, plus a zero-mean random component, ϵ, that follows a particular probability distribution. That is,

$$Y = \phi(X; \Theta) + \epsilon \tag{4}$$

The addition of the random term makes the above relationship a statistical model, meaning that the functional relationship between the response variable Y and the predictor variable X holds only in an average sense, not for every data point. Based on the experimental results in previous section, it seems reasonable to assume a linear form for the regression function $\phi(\cdot)$ where $\Theta = (\alpha_1, \alpha_2)$ when Y represents ΔK and $\Theta = (\beta_1, \beta_2)$ when Y represents da/dN.

To complete the model, the error term ϵ must be fully specified as well. Here we adopt the classic regression assumption that the errors are independent and identically-distributed (i.i.d.) random variables and follow a normal probability distribution:

$$\epsilon \sim N(0, \sigma) \tag{5}$$

The mean of the error distribution is zero, and its standard deviation is the unknown parameter σ. Another classic assumption in regression analysis is that the error has a constant variance for all observations regardless of the value of independent variable X. In this application, however, it is reasonable to assume that a small crack is harder to measure, and as the crack becomes larger, the measurement

of its length becomes more accurate. Accordingly, the da/dN and ΔK values associated with data points coming from smaller cracks could be less accurate than those from larger cracks.

One way to account for this effect is to release the constant variance assumption and allow σ to change as a function of the independent variable X. This will result in a flexible model that can capture any change in the error distribution based on the available data. Here, we choose a flexible two-parameter exponential relationship to capture the potential trend in σ,

$$\sigma = \gamma_1 \exp(\gamma_2 X) \tag{6}$$

This function can capture both increasing and decreasing trends of σ for positive and negative values of γ_2, respectively. It also reduces to the standard constant variance case if γ_2 is equal to zero. It is important to note that it is not necessary to have any prior knowledge about the trend of σ; γ_1 and γ_2 are in fact treated as additional unknown parameters and will be estimated using the observed data.

2.3. Bayesian parameter estimation

Numerous procedures have been developed for parameter estimation and inference in regression analysis. Here we adopt a Bayesian approach to parameter estimation often referred to as *Bayesian regression*.

In Bayesian inference, the initial belief about the distribution of the parameters (*a priori* distribution) is systematically updated according to Bayes' theorem (Eq. (7)), based on some kind of evidence or available observations (Figure 4).

$$p(\Theta|D) = \frac{p(D|\Theta)p(\Theta)}{p(D)} \tag{7}$$

where Θ is the vector of model parameters to be estimated and D denotes the set observations to be used in the updating process. $p(\Theta)$ is the *a priori* distribution of model parameters while $p(\Theta|D)$ is the *a posteriori* probability of the model parameters once updated by the observations.
The model that was developed in the previous section can be summarized in the following form:

$$Y = \alpha_1 X + \alpha_2 + \epsilon$$

where

$$\epsilon \sim N(0, \sigma), \tag{8}$$

$$\sigma = \gamma_1 \exp(\gamma_2 X)$$

The likelihood can be defined based on the distribution of the error term, ϵ. To do so, the error $\epsilon_i = y_i - (\alpha_1 x_i + \alpha_2)$ for every data point (x_i, y_i) is calculated.
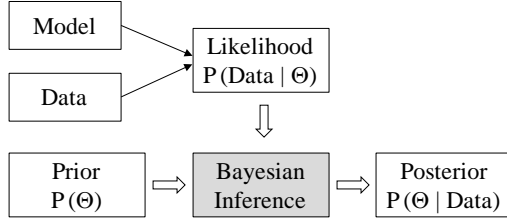
Figure 4: Bayesian Inference Framework

Next, the likelihood of each data point can be defined according to $\epsilon_i \sim N(0, \gamma_1 \exp(\gamma_2 x_i))$. This can be written explicitly as,

$$p(D|\alpha_1, \alpha_2, \gamma_1, \gamma_2)$$
$$= \prod_{i=1}^{n} \frac{1}{\sqrt{2\pi}\sigma} \exp\left(-\frac{1}{2}\left(\frac{y_i - (\alpha_1 x_i + \alpha_2)}{\gamma_1 \exp(\gamma_2 x_i)}\right)^2\right) \quad (9)$$

The likelihood in Eq. (9) is based on the assumption that the data points are independent and therefore the likelihood for dataset D is simply the multiplication of the likelihood function for every data point.

This study began with no past experience, and therefore non-informative (uniform) prior distributions for all parameters $\alpha_1, \alpha_2, \gamma_1$ and γ_2 were chosen.

The denominator in Bayes' theorem acts as a normalization factor and can be written as,

$$p(D) = \int p(D|\Theta)p(\Theta)d\Theta \quad (10)$$

In practice, numerical approaches such as Monte Carlo-based methods are used to calculate the multidimensional integral in Eq. (10). Here we used WinBUGS (Cowles 2004) to obtain the posterior distributions; WinBUGS is a software package for Bayesian analysis of complex statistical models using Markov chain Monte Carlo (MCMC) methods. Interested readers can refer to (Ntzoufras 2009) for a good reference on Bayesian modeling using WinBUGS. For further reading on MCMC methods in general, see (Gelman et al. 2003; Gamerman & Lopes 2006).

Once the posterior distribution $p(\Theta|D)$ is calculated, the inference process is complete. The next step is to use the developed model for prediction using unobserved data. In other words, the model (with posterior parameters) will be used to calculate the distribution of dependent variable Y for a given input X.

The posterior *predictive distribution* is the distribution of unobserved observations (prediction) conditional on the observed data. Let D be the observed data, Θ be the vector of parameters, and D_{pred} be the unobserved data; the posterior predictive distribution is defined as follows,

$$p(D_{pred}|D) = \int p(D_{pred}|\Theta)p(\Theta|D)d\Theta \quad (11)$$

Here again, we are dealing with a multi-dimensional integral that should be calculated numerically. The same MCMC procedure described above can be used to generate samples from the posterior predictive distribution based on draws from the posterior distribution of Θ.

2.3.1. Parameter estimation results

Figure 5 shows the contour plot of the posterior joint distribution of parameters α_1 and α_2. The figure shows that these two parameters are highly correlated (Correlation coefficient $\rho = -0.88$). Similar results are presented in Figure 6 for the parameters γ_1 and γ_2. These variables are also highly correlated ($\rho = -0.89$), which highlights the importance of considering their joint distribution (rather than marginal distributions) when using the model for prediction.
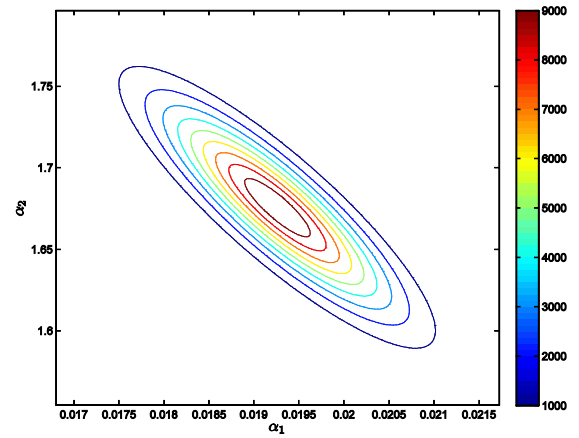
Figure 5: Contour plot of the posterior joint distribution of parameters α_1 and α_2.
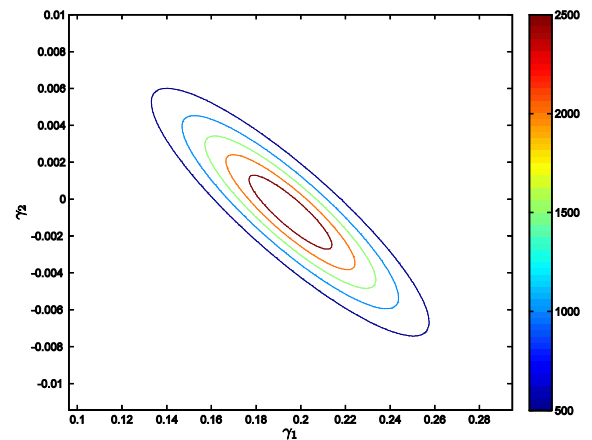
Figure 6: Contour plot of the posterior joint distribution of parameters γ_1 and γ_2.

It was previously described that the flexible model in Eq. (6) was used to define the standard deviation of the dependent variable Y. For any given input X, one can calculate the corresponding distribution of σ by knowing the joint distribution of γ_1 and γ_2 which was one of the outcomes of the parameter estimation process. This result is shown in Figure 7. Note that for this particular dataset, the median value of σ is relatively constant (it has a slight decreasing trend) over the range of values of $\log dc/dN$. This is consistent with the fact that the estimated value of γ_2 is close to zero (see Figure 6), which means that the relationship in Eq. (6) reduces to a constant variance case where $\sigma_{\Delta K} \approx \gamma_1$. Notice the change in the calculated bounds of σ over the range of $\log dc/dN$. The tighter bounds in the middle of the range are due to a higher density of data points in this region, which results in a more confident estimate in this range.
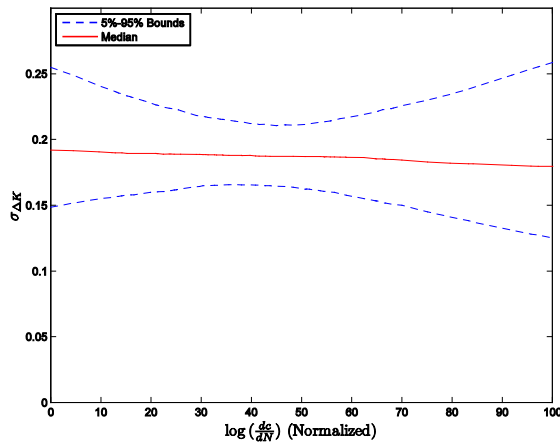

Figure 7: Distribution of $\sigma_{\Delta K}$ as a function of the independent variable $\log dc/dN$
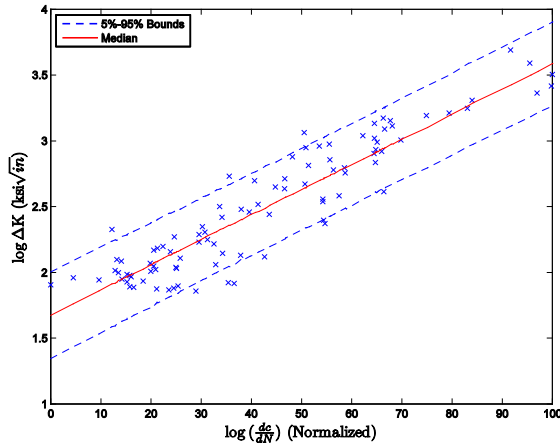

Figure 8: Posterior predictive distribution of $\log \Delta K$ as a function of $\log dc/dN$

Once all the model parameters are estimated, Eq. (11) can be used to calculate the posterior predictive distribution for the dependent variable $\log \Delta K$ as a function of the independent variable $\log dc/dN$, given past observations, D. The result is presented in Figure 8 where the posterior distribution is shown by its median and the 5% and 95% prediction bounds.

The procedure described above can be repeated to fit the model in Eq. (8) to the $\log da/dN$ versus $\log dc/dN$ dataset as well. The models developed in this section provide a quantitative means for relating the crack growth parameters to the AE parameters. In the remainder of this paper, this concept will be used to develop a complete SHM solution based on AE monitoring.

3. STRUCTURAL HEALTH MANAGEMENT USING AE

Three novel approaches are proposed for structural health management using AE monitoring. In all of these approaches, the statistical model developed in the previous section will be utilized to calculate system health parameters solely based on AE monitoring data.

3.1. AE-based damage severity assessment

In this section, we will calculate the probability of structural failure (as defined here) due to crack growth using AE monitoring data.

As a crack grows in a structure, the value of the stress intensity factor ΔK associated with it increases as well. For a standard CT specimen, this relationship is defined as follows (ASTM E647-08 2008):

$$\begin{aligned} \Delta K &= f(a) \\ &= \frac{\Delta P}{B\sqrt{W}} \frac{2\alpha}{(1-\alpha)^{3/2}} (0.886 + 4.64\alpha \\ &\quad - 13.32\alpha^2 + 14.72\alpha^3 - 5.6\alpha^4) \end{aligned} \quad (12)$$

where ΔP is the range of the applied force cycles, W and B are the width and thickness of the CT specimen, respectively, and α is the dimensionless crack size defined as a/W. Equation (12) shows that ΔK, in general, depends on the geometry of the structure, amplitude of the applied load cycles and the instantaneous size of the crack. For a given structure, assuming that the geometry is fixed, a large ΔK represents either a large crack size and/or high load amplitude applied to the structure. ΔK can therefore be considered a criticality parameter that describes the potential of the crack for further growth at any given point in time.

On the other hand, the resistance of a material to stable crack propagation under cyclic loading is characterized by its fracture toughness, K_{Ic} (Anderson 1994). At any point during the crack growth, if the stress intensity exceeds the fracture toughness of the material, the crack growth transitions from stable to non-stable/rapid growth regime where failure is imminent (Figure 9).
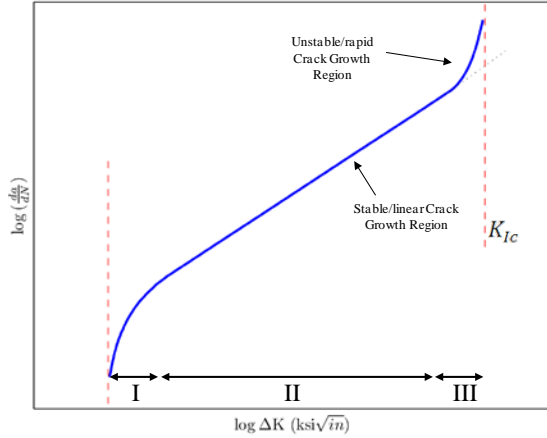
Figure 9: Crack growth sigmoid curve showing both stable and unstable crack growth regions.

In other words, the crack growth is stable as long as K_{max} is less than the fracture toughness of the material, K_{Ic}. This fact is used to define an AE-based measure of risk, R_{AE}, as follows,

$$R_{AE} = p(K_{max} > K_{Ic}) \qquad (13)$$

where K_{max} is defined according to Eq. (12) for $\Delta P = P_{max}$.

Our objective is to assess the health of the structure based only on AE monitoring. To do so, the statistical model developed previously is used in the following way:

Step 1: Estimate the model parameters (Θ) using experimental data for a given structure,

Step 2: Monitor the structure using the AE technique and extract the dc/dN parameter from the observed signals,

Step 3: At any given time, use Eq. (11) to calculate the posterior predictive distribution of ΔK as a function of instantaneous AE parameter, dc/dN.

Step 4: Use Eq. (13) to calculate R_{AE} (noting that $K_{max} = \Delta K/(1 - R)$ for constant amplitude loading with loading ratio R).

Figure 10 shows the outcome of the above procedure for steps 1-3. The structure is monitored using the AE technique, and the dc/dN feature is extracted from the signals at different values of elapsed cycles, N. At any given cycle N, the posterior predictive distribution as a function of the instantaneous AE feature, dc/dN, can be calculated. As the number of cycles increases, the crack continues to grow, and therefore, the distribution of K_{max} gradually shifts towards larger values.

Following step 4 in the procedure described above, R_{AE} can be calculated for any given cycle N according to Eq. (13). The result is shown in Figure 11. As shown in this figure, R_{AE} increases (non-monotonically) throughout the experiment.
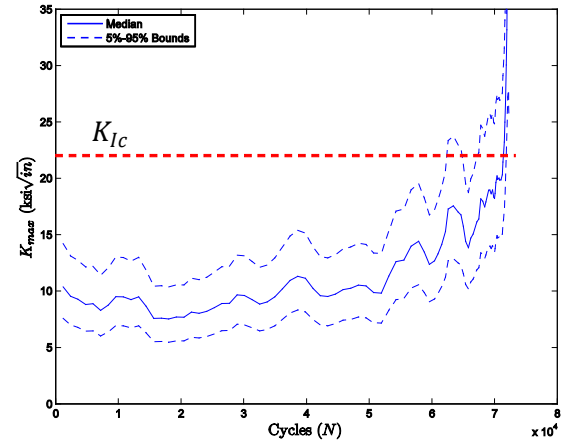

Figure 10: Probability distribution of K_{max} as a function of applied fatigue cycles, N
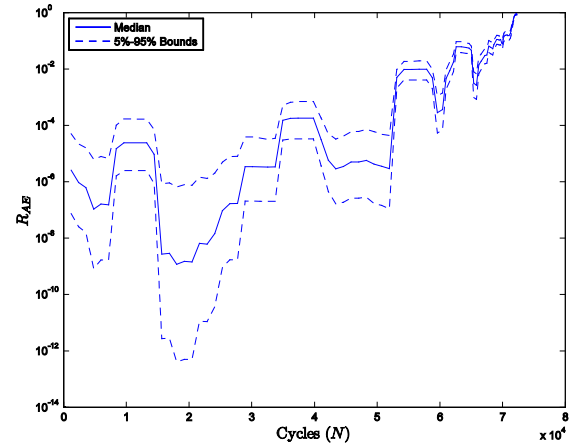

Figure 11: AE-based risk factor, R_{AE}, calculated as a function of applied fatigue cycles, N

The fluctuations in this figure are in fact a direct result of the fluctuations in the input AE feature, dc/dN, which also matches the trend in Figure 10. The AE-based risk factor defined here is an *instantaneous* exceedance probability calculated based on the average value of dc/dN for any given interval. The AE feature has an overall increasing trend that may fluctuate due to instantaneous dynamics of the crack growth. So the best way to interpret the result in Figure 11 is to treat it as a red/green warning mechanism to alert the decision-maker in real-time about the increased risk factor at a given cycle based on the current AE readings.

3.2. AE-based crack growth model

For a given initial crack size, if the rate of crack growth can be estimated, then the crack size itself can be easily calculated by a summation over crack size increments starting from the known initial size. This is the logic behind

most crack growth models. In these models, however, the rate of crack growth is usually calculated based on its empirical relationship with the ΔK parameter, which itself has a complex derivation even for simple geometries.

In the approach presented here, the rate of crack growth is estimated directly from AE monitoring using the statistical model that was developed earlier. The process of estimating crack size using this AE-based crack growth model is summarized in Figure 12.
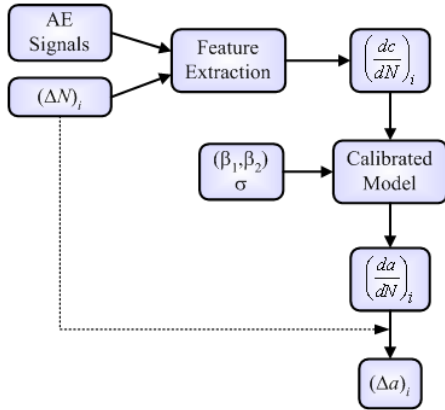

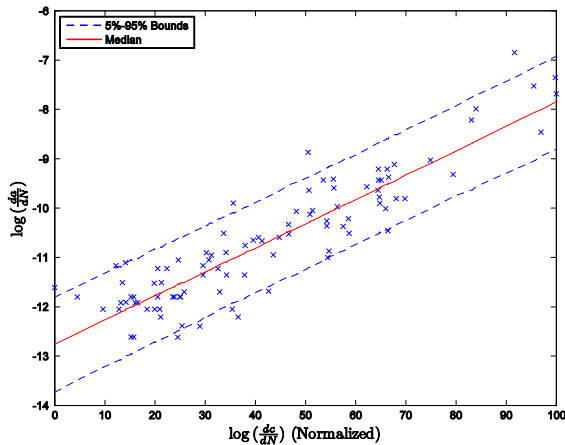Figure 12: Flowchart of the AE-based crack growth model (Rabiei et al. 2010)

Figure 13: Posterior predictive distribution of $\log da/dN$ as a function of $\log dc/dN$

The process starts by finding the parameters of the model in Eq. (8), where $Y = \log da/dN$ and $X = \log dc/dN$, based on relevant experimental data. The resulting posterior predictive distribution will be used to estimate the distribution of da/dN for any given input dc/dN.

Consider a crack growth experiment where crack growth-related AE signals are recorded throughout the test. For any given interval of elapsed cycles, ΔN_i, the corresponding average AE feature $(\Delta c/\Delta N)_i$ can be calculated. Figure 14 shows the feature extracted from such data during crack

growth in a CT specimen. The probability distribution of the crack extension Δa_i corresponding to the interval ΔN_i can be calculated using Eq. (11). This is shown in Figure 15 using the input AE data shown in Figure 14 and the calibrated model shown in Figure 13.
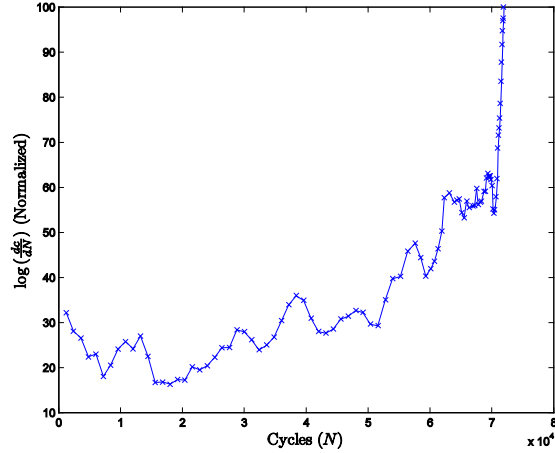

Figure 14: The AE count rate feature extracted from signals obtained during crack growth in a CT specimen
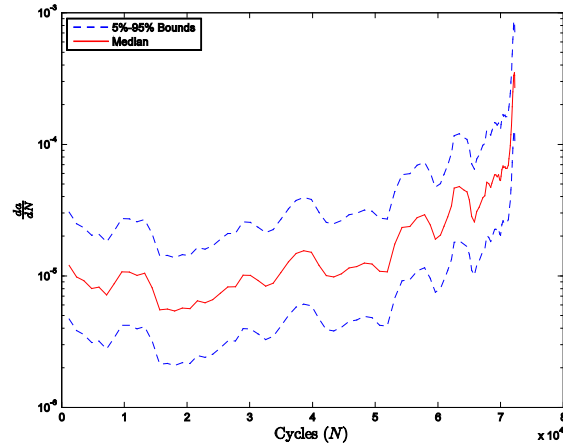

Figure 15: Crack growth rate as a function of applied fatigue cycles predicted via AE monitoring

If the crack size is known at the beginning of the interval, a probability distribution for the crack size at the end of the interval can be easily obtained. By repeating this process for consecutive intervals, multiple crack growth trajectories can be generated, as shown in Figure 16.

The main feature of the AE-based crack growth model presented here is that the rate of crack growth is determined experimentally, and therefore, there is no need to have any information about the amplitude of the applied loading cycles to the structure. This approach, however, relies heavily on a calibrated statistical model that should describe the relationship between an NDI feature of interest

($\log dc/dN$ in this case) and the crack growth rate. Developing a robust model that can capture this relationship with minimum uncertainty is a difficult task that is still a topic of continued research.
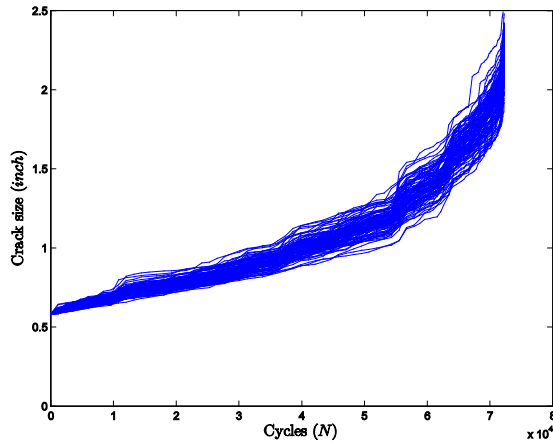

Figure 16: Crack growth trajectories obtained via AE-based crack growth model

3.3. Bayesian knowledge fusion

So far two approaches have been proposed to use AE for quantitative structural health management. A third approach will be discussed here which seeks to use AE findings as an independent source of information to update the outcome of empirical crack growth models.

Several models of varying complexity, e.g. (Forman et al. 1997) and (Walker 1970), have been proposed to describe the crack growth phenomenon. The outcomes of these models suffer from uncertainty from various sources including material properties, model parameters and the model structure. Despite all efforts to capture various sources of uncertainty, the final outcome of the empirical models could still be far from true crack size.

Consider the crack growth test described earlier in this paper. Figure 17 shows the true crack growth trajectory along with empirical model prediction for the CT specimen being considered here. The model in this case consistently underestimates the true crack size. This shows that the actual crack growth rate in the experiment was higher than what was predicted by the model. Several factors (including uncertainty in model structure, uncertainty in model parameters or presence of rogue flaw) could contribute to the poor performance of the empirical model. It is therefore highly desirable to update the model estimates using an independent source of information.

Using the statistical model presented earlier, the AE signals can be translated into crack growth rate information and be used to update the empirical model prediction. (Rabiei 2011) proposed an efficient Bayesian framework to

recursively update the empirical model prediction as well as the model parameters using crack growth rate and crack size observations.
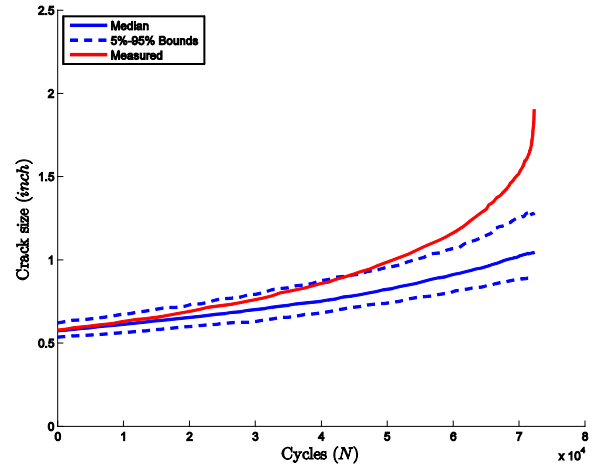

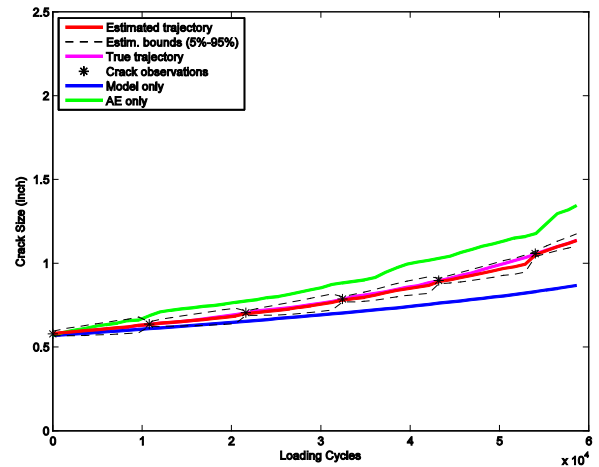Figure 17: Probabilistic crack growth simulation result using empirical model

Figure 18: Recursive Bayesian estimation of crack size using crack size and AE-based crack growth rate observations

In Figure 18 the updated crack size estimate for the specimen described above is presented. This result is obtained by: a) recursively updating the crack growth rate based on the AE data, and b) updating crack size at fixed intervals using crack size observations (e.g. periodic inspections). In this figure, the line marked as *model only* is the outcome of the empirical crack growth model. The *AE only* line, on the other hand, shows the crack growth trajectory as predicted solely by the AE-based crack growth model. The *estimated trajectory* is the fusion result obtained via recursive Bayesian estimation. In this particular case, since the empirical model consistently underestimates while

9

the AE-based approach consistently overestimates the crack size, the fusion results in an enhanced crack size prediction. It is important to note that this observation is based on results from limited experimentation and cannot be generalized. The fusion outcome is dependent on the performance of the individual techniques fused together. Obviously, if both the model and the AE observations overestimate the crack size in one application, the fused result will also be an overestimation of the true crack trajectory.

4. CONCLUSION

Three new approaches were proposed for quantitative structural health management using in-situ AE monitoring: in the first approach, an AE-based risk measure, R_{AE}, was defined as the probability that the crack growth will transition from the stable to non-stable/rapid growth regime. The transition probability was calculated as the probability that K_{max} exceeds the fracture toughness of the material, K_{Ic}. In the proposed approach, K_{max} is calculated as a function of real-time AE monitoring data using the calibrated statistical model developed in this paper.

In the second approach, AE monitoring data was used to calculate the instantaneous distribution of crack growth rate, da/dN. For a given initial crack size and with crack growth rates obtained from AE monitoring, the crack size distribution was estimated as a function of elapsed fatigue cycles.

Recursive Bayesian estimation technique was used to fuse the outcome of the empirical crack growth model with crack size observations as well as the online crack growth rate observations obtained from AE monitoring.

5. REFERENCES

Anderson, T.L., 1994. *Fracture Mechanics: Fundamentals and Applications, Second Edition* 2nd ed., CRC.

ASTM E647-08, 2008. *Standard Test Method for Measurement of Fatigue Crack Growth Rates*, ASTM International.

Bassim, M.N., St Lawrence, S. & Liu, C.D., 1994. Detection of the onset of fatigue crack growth in rail steels using acoustic emission. *Engineering Fracture Mechanics*, 47(2), pp.207-214.

Cowles, M.K., 2004. Review of WinBUGS 1.4. *The American Statistician*, 58(4), p.330–336.

Forman, R.G., Kearney, V.E. & Engle, R.M., 1997. Numerical analysis of crack propagation in cyclic-loaded structures.

Gamerman, D. & Lopes, H.F., 2006. *Markov chain Monte Carlo: stochastic simulation for Bayesian inference*, Chapman & Hall/CRC.

Gelman, A. et al., 2003. *Bayesian Data Analysis, Second Edition* 2nd ed., Chapman & Hall.

Hamel, F., Bailon, J.P. & Bassim, M.N., 1981. Acoustic emission mechanisms during high-cycle fatigue. *Engineering Fracture Mechanics*, 14(4), pp.853-860.

Holford, K.M. et al., 2009. Acoustic emission for monitoring aircraft structures. *Proceedings of the Institution of Mechanical Engineers, Part G: Journal of Aerospace Engineering*, 223(5), pp.525-532.

Mix, P.E., 2005. *Introduction to nondestructive testing: a training guide*, Wiley-Interscience.

Ntzoufras, I., 2009. *Bayesian Modeling Using WinBUGS*, Wiley.

Paris, P. & Erdogan, F., 1963. A critical analysis of crack propagation laws. *Journal of Basic Engineering*, 85(4), p.528–534.

Rabiei, M., 2011. *A Bayesian framework for structural health management using acoustic emission monitoring and periodic inspections*. College Park: University of Maryland.

Rabiei, M., Modarres, M. & Hoffman, P., 2009. Probabilistic Structural Health Monitoring Using Acoustic Emission. In Annual Conference of the Prognostics and Health Management Society 2009. San Diego, CA.

Rabiei, M., Modarres, M. & Hoffman, P., 2010. Towards Real-Time Quantification of Fatigue Damage in Metallic Structures. In Aircraft Airworthiness & Sustainment (AA&S 2010). Austin, TX.

Rahman, S. & Rao, B.N., 2002. Probabilistic fracture mechanics by Galerkin meshless methods–part II: reliability analysis. *Computational mechanics*, 28(5), p.365–374.

Walker, K., 1970. The effect of stress ratio during crack propagation and fatigue for 2024-T3 and 7075-T6 aluminum. *Effects of environment and complex load history on fatigue life*, p.1–14.